

RESEARCH ARTICLE

Intensified variability of the El Niño–Southern Oscillation enhances its modulations on tree growths in southeastern China over the past 218 years

Lei Wang¹  | Keyan Fang^{1,2} | Dai Chen³ | Zhipeng Dong¹ | Feifei Zhou¹ | Yingjun Li¹ | Peng Zhang⁴ | Tinghai Ou² | Guoyang Guo¹ | Xinguang Cao^{1,5} | Mingtong Yu¹

¹Institute of Geography, Key Laboratory of Humid Subtropical Eco-geographical Process (Ministry of Education), College of Geographical Sciences, Fujian Normal University, Fuzhou, China

²Regional Climate Group, Department of Earth Sciences, University of Gothenburg, Gothenburg, Sweden

³International Forestry Cooperation Center, State Forestry Administration, Beijing, China

⁴Department of Oceanography, Chonnam National University, Gwangju, South Korea

⁵Institute of Geography and Resources of Dabie Mountains, College of Tourism Culture and Geographical Sciences, Huanggang Normal University, Huanggang, China

Correspondence

Keyan Fang, Institute of Geography, Key Laboratory of Humid Subtropical Eco-geographical Process (Ministry of Education), College of Geographical Sciences, Fujian Normal University, Fuzhou 350004, China.
Email: kfang@fjnu.edu.cn

Funding information

non-profit project of Fujian province, Grant/Award Number: 2015R1034-2, 2015R1034-8; the Fellowship for Distinguished Young Scholars of Fujian Province, Grant/Award Number: NO. 2015J06008; the National Science Foundation of China, Grant/Award Number: U1405231, 41471172, 91537210

Lack of long-term tree-ring records in the core regions of the Asian summer monsoon in southeastern China limits our ability of evaluating the current climate change in a historical context. In this study, we developed the first 218-year tree-ring chronology (1798–2015) of *Pinus massoniana* in Zhangping area, Fujian Province, humid subtropical China. This chronology is positively correlated with winter–spring (January–March) temperature ($r = 0.359$, $p < .01$) and summer (July–September) precipitation ($r = 0.351$, $p < .01$). Although the correlations between our tree rings with sea surface temperatures (SSTs) are not very high, the correlation pattern is very close to the correlation pattern with the El Niño–Southern Oscillation variability (ENSO). These suggest that the ENSO could be the major large-scale regulator on the growth of our tree rings. The strength of the correlations between our tree rings and the ENSO ($r = 0.30$, $N = 66$) matches closely with the ENSO variability during 1950–2015. The modulations of the ENSO on regional tree growth have been the most conspicuous since the 1950s, which corresponds to its enhanced inter-annual variability. The extreme growth anomalies match quite well with the extreme years of the moisture-sensitive chronologies. The dry epoch from 1935 to 1958 is the most severe long-lasting drought in our tree rings, which is a widely distributed pattern in southeastern China and is likely modulated by the La Niña-like modes in that period.

KEYWORDS

ENSO, inter-annual variability, southeast China, tree rings

1 | INTRODUCTION

Climate variability at inter-annual (1–10 years) and inter-decadal (10–100 years) scales are key concerns for both the scientific community and the public, because these time-scales are closely related to livelihood and economic sustainable developments (Hartmann *et al.*, 2013). The instrumental data in China mostly started in the 1950s. This limits our ability of understanding the inter-annual and inter-decadal climate variability before the 1950s when the influences of the anthropogenic activities were weaker than the

present. Therefore, it is crucial to extend the instrumental records back into centuries. Tree-ring is an invaluable biological proxy that takes advantages of both instrumental and geological data in some extent. Relative to the instrumental data, it is longer and can be extended back to the pre-industrial periods. Relative to the geological data, it often has higher resolution and is more accurately dated and can be better calibrated with instrumental data. These advantages allow us to employ the diagnostic tools in atmospheric sciences to study its temporal features and the underlying climate regimes (Fang *et al.*, 2014b; 2015). In addition to these

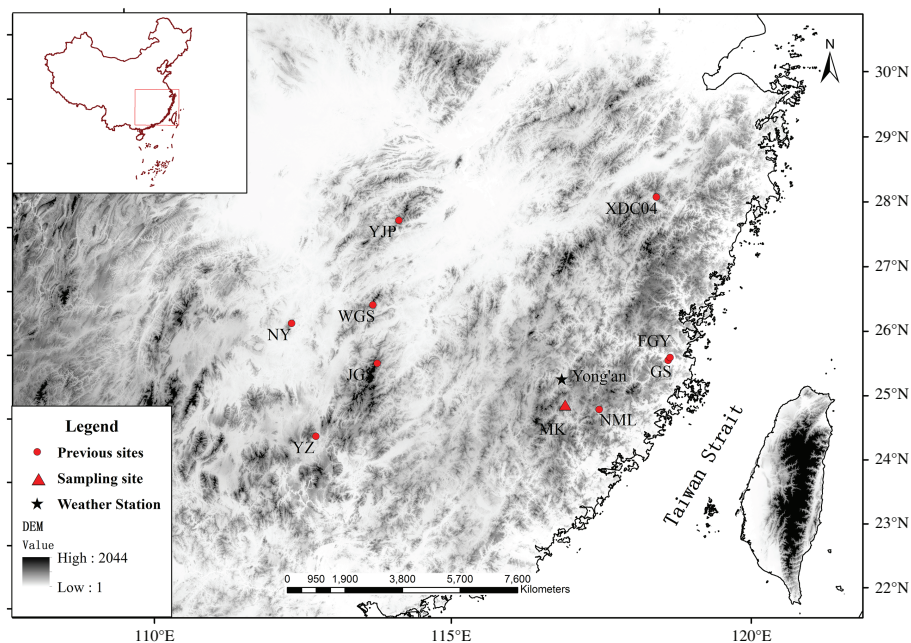


FIGURE 1 Locations of our sampling site Makeng (red triangle), the locations of the published tree-ring sites (red rounds) in southeastern China and Yong'an meteorological station (black star). The Bidoup Nui Ba National Park (BDNP) site is not shown since the limiting typesetting [Colour figure can be viewed at wileyonlinelibrary.com]

temporal features, it is widely and densely distributed and allows the detection of spatial features. Given these advantages, long-term tree-ring data have been widely used to infer the spatiotemporal variations of climate in China, particularly for its cold and arid northwestern part (Liang *et al.*, 2006; Shao *et al.*, 2010; Wang *et al.*, 2011; Yang *et al.*, 2014; Gou *et al.*, 2015; Liu *et al.*, 2014; Zhang *et al.*, 2015). However, only a few tree-ring-based climate proxies have been presented for the hot and humid southeastern China (Chen *et al.*, 2012a; 2012b; 2012c; Li *et al.*, 2016).

We hypothesize that tree rings in hot and humid regions such as southeastern China are expected to provide more information on the oceanic and atmospheric modes, such as the El Niño–Southern Oscillation (ENSO) variability (Allan *et al.*, 1996), because the hot and humid regions, such as southeastern China, are closer to the ocean or are more influenced by the oceanic factors than the cold and arid regions. Indeed, the tree-ring data from some hot and humid regions, such as Indochina, showed high correlations with ENSO (Buckley *et al.*, 2010). On the other hand, developments of long-term tree-ring proxies in southeastern China can help to generate a full picture of the Asian monsoon as they are located in the core areas of the Asian summer monsoon.

In this study, we developed a 218-year tree-ring width chronology for *Pinus massoniana* in Fujian province, southeastern China. With the use of this chronology, we aim to (a) reveal the relationships between tree growth and local climate and (b) the linkages between tree growth and oceanic and atmospheric modes.

2 | MATERIALS AND METHODS

2.1 | Study area

The study area is located in Zhangping county of Fujian province in southeastern China. The sampling site of Makeng (MK) (25°34'N, 117°21'E, 1,000 m a.s.l.) is located in the stretching branch of the Daiyun Mountain, the highest mountain of central Fujian province (Figure 1). It has a humid subtropical monsoon climate. The mean annual temperature of the study region is 19.5 °C and the mean annual total precipitation is 1,545 mm according to the meteorological records from the Yong'an station (25°58'N, 117°21'E, 206 m a.s.l., 1954–2015). The mean monthly temperature ranges from 9.4 °C in January to 28.3 °C in July. While the temperature in July and August are the hottest months, the precipitation is about half of that in May and June (Figure S1, Supporting Information). In general, it is cool and humid for late spring and hot and dry for summer (Chen *et al.*, 2015). The study region is covered by the yellow soil, which is rich in organic matter. The MK sampling site is dominated by Masson pine (*P. massoniana*) trees, mixed with bamboo and broadleaf–coniferous forests.

2.2 | Tree-ring data

Two to three tree-ring cores were taken from the breast height of 45 old living *P. massoniana* trees. The samples were mounted, air dried and smoothed with sand-paper until the cellular structure could be clearly identified (Stokes and Smiley, 1968). Each core was cross-dated, assigning each

ring to calendar years by checking the total matches of the growth patterns of the tree-ring widths. The cross-dated series were measured to an accuracy of 0.001 mm using a LINTAB 6.0 measuring station. The quality of cross-dating was checked using the program COFECHA (Holmes, 1983). The poor quality samples which were broken seriously were abandoned. Overall, 56 tree-ring series out of 34 trees from the total 96 samples were selected for further analysis.

In order to remove the age-related growth trends in the tree-ring data, the measured tree-ring series were fitted by a smoothed cubic spline curve with two-thirds of the mean lengths of each series. The detrended tree-ring indices were then averaged to produce the standard chronology following the biweight robust mean method (Cook, 1985) by the ARSTAN program (Cook *et al.*, 2003). To account for the decrease in sample size back in time, we used the statistic of the sub-sample signal strength (SSS) higher than 0.85 to determine the reliable portion of the tree-ring chronology (Wigley *et al.*, 1984).

2.3 | Climate data

The instrumental data of monthly temperature and precipitation in Yong'an station were obtained from China Meteorological Data Center (<http://data.cma.gov.cn/>). The weather station is approximately 46 km from our sampling site with the data starting from 1954. Our sampling site locates in the stretch of the highest mountain in Fujian without obstruction of mountains between our site and Pacific Ocean which may response to the oceanic and atmospheric modes better. This study uses the monthly sea surface temperature (SST) data from the Hadley Centre Global Sea Ice and Sea Surface Temperature (HadISST; Rayner *et al.*, 2003). We use SST averaged over the equatorial Pacific (Niño3: 5°S–5°N, 150°–90°W; Niño3.4: 5°S–5°N, 170°–120°W; Niño4: 5°S–5°N, 160°E–150°W) to track ENSO, which is referred to as the ENSO index. The SST data are more reliable since 1950 (Du and Xie, 2008; Xie *et al.*, 2010). We employed the geopotential heights (GPH) data from the reanalysis product of the National Centers for Environmental Prediction–National Center for Atmospheric Research (NCEP–NCAR; Kalnay *et al.*, 1996). Only the GPH data since 1968 have been used in this study because of the low data quality over Asia prior to 1968 (Yang *et al.*, 2002). The Pacific Decadal Oscillation (PDO) from 1907 to 2015 were the time series of the first principal component obtained by EOF of SST northwards of 20°N in the North Pacific, which are available online at http://climexp.knmi.nl/data/ipdo_hadsst3.dat (Kennedy *et al.*, 2011).

The Atlantic Multidecadal Oscillation (AMO) index used for comparison data set is obtained from http://climexp.knmi.nl/data/iamo_hadsst.dat.

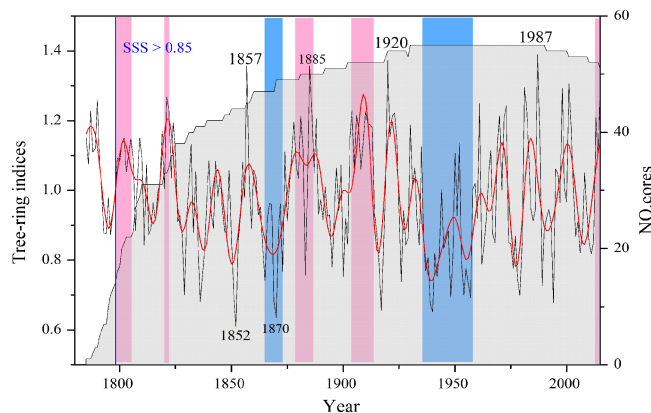


FIGURE 2 Time series of tree-ring standard chronology (black line), the 10-year low-passed data of the standard chronology (red bold line) and the sample size (shadow region) developed from *P. massoniana* of Makeng from 1785 to 2015. 1867, 1885, 1920 and 1987 are extremely high values ($>\text{mean} + 2\text{SD}$) of standard chronology, 1852 and 1870 extremely low values ($<\text{mean} - 2\text{SD}$). The (pink shaded area) error ranges were derived from the signal strength of the 20-year low-passed data [Colour figure can be viewed at wileyonlinelibrary.com]

2.4 | Methods

Because tree growth may be influenced by climate condition of previous year, the climate–growth correlations between observed monthly climate variables from Yong'an meteorological station and the tree-ring width chronology were calculated from last January to current December. The running correlations were calculated with a 21-year moving window to study the time-varying relationships. The first-order differenced data were calculated as the residual of the values of consecutive years. The first-order differenced data can highlight the inter-annual variability of the time series. The correlations between the chronology with ENSO indices of the Niño3, Niño3.4 and Niño4 are calculated, respectively.

3 | RESULTS

3.1 | Tree-ring chronology

The mean segment length of the tree-ring series is ~140 years. The tree-ring chronology spans from 1785 to 2015 based on 56 cores from 32 trees and its reliable portion started in 1798 when over 14 series are available (Figure 2). Extremely high values ($>\text{mean} + 2\text{SD}$) are observed in years of 1857, 1885, 1920 and 1987 and extremely low values ($<\text{mean} - 2\text{SD}$) are seen in year of 1852 and 1870 (Table 1). Continuously high growth values ($>\text{mean} + 1\text{SD}$) for the low-passed data (>10 years) of the chronology are observed in periods during 1798–1804, 1819–1821, 1879–1888, 1903–1913 and 2013–2015 and low growth values ($<\text{mean} - 1\text{SD}$) are seen in periods during 1865–1873 and 1935–1958 (Table 2 and Figure 2).

TABLE 1 The comparison of extreme positive and negative years of standard chronologies

Extreme year (MK)		Source					
Positive	Negative	BDNP	XDC04	RC	NML	GS	FGY
	1852	/					/
1857							
	1870						✓
1885		✓	✓				✓
1920		✓					
1987		✓					

Note. / represents no data in this year. BDNP = Bidoup Nui Ba National Park site, the BDNP chronology multiplied by negative one (Buckley *et al.*, 2010); FGY = Fangguangyan site (Guo *et al.*, 2018); GS = Gushan site (Li *et al.*, 2016); NML = Niumulin site (Li *et al.*, 2017); RC = regionally composite sites (Duan *et al.*, 2011); XDC04 = a chronology in nearby Zhejiang province (Shi *et al.*, 2015).

3.2 | Climate–growth relationships

Significant positive correlations are found between tree growth and temperature in previous January, March, current February, March and October at the $p < .05$ level of significance (Figure 3a). The highest correlation ($r = 0.36$, $p < .01$) with seasonal temperature was found in winter–spring from current January to March followed by from current January to October ($r = 0.34$, $p < .01$). Tree growths are positively and significantly correlated with precipitation in current summer–autumn (July–September) ($r = 0.35$, $p < .01$). As shown in Figure 3b, correlations among the tree-ring indices, precipitation and temperature based on first-order differenced data are similar to the correlations calculated from the raw data. Slight differences are seen that the correlation between tree ring and temperature from January to October is higher than the correlation from January to March and the highest correlation with precipitation was in July. Taken together, tree growths are mainly controlled by the temperature in winter–spring and the precipitation in summer.

Figure 4a shows that tree growths are positively correlated with the SST in eastern equatorial Pacific and negatively correlated with SST in the western Pacific Ocean. The correlation pattern resembles an El Niño pattern of sea surface temperature anomalies in the tropical Pacific (Allan

et al., 1996; Sturman, 2010), suggestive of the potential modulations of ENSO on our tree rings. Note that tree growths are also positively correlated with the SST in the tropical Indian Ocean. These suggest that the Indian SST may be an important factor linking the ENSO and climate of our study region. Indian SST plays a crucial role in modulating the strength of the Indian summer monsoon, which influences summer climate over most of southern China including our study region. On the other hand, the Indian SST is closely linked to the ENSO. For example, in response to the ENSO matured in winter, the Indian Ocean often has a capacitor effect that can store the ENSO signal till summer and cause anomalies in Indian summer monsoon (Xie *et al.*, 2003; 2010). It is also possible that the Indian SST alone may also strongly influence our study region as it is a key regulator for the Indian summer monsoon. The correlations between the first-order differenced data are similar but much stronger, which indicates the modulations of El Niño on regional tree growths are more conspicuous at short timescales (1–10 years). As is shown in Figure 4c, the El Niño-like correlation pattern is more significant when the correlations ($r = 0.30$, $N = 66$) with SST have been calculated during the period since 1950 because the quality of the SST data is more robust (Xie *et al.*, 2010). The highest correlations ($r = 0.44$, $N = 65$) with the El Niño-like correlation pattern have been observed for the first-order differenced data during their common period since 1950 (Figure 4d).

Although the correlations with SST and the ENSO indices are not high, the spatial correlation pattern is very similar to the correlation pattern between the ENSO and SST. Because limited correlations with SST are not related to the ENSO, we conclude that the ENSO is the major regulator on tree growths of this region. Moderately high correlations with regional climate and the ENSO may be due to the growth disturbances. For example, higher correlations with regional climate and the SST are found for the first-order differenced data, which reflect the correlations at short timescales (1–10 years). This agrees with the notion that the growth disturbances play a less influential role on tree growth at short timescales relative to the inter-decadal timescales (Fang *et al.*, 2017).

TABLE 2 The comparison of extreme positive and negative years based on 20-year low-passed data of seven standard chronologies

Extreme periods (MK)							
Positive	Negative	BDNP (1304)	XDC04 (1856)	RC (1851)	NML (1836)	GS (1804)	FGY (1853)
1798–1804							
1819–1821							
	1865–1873					✓	✓
1879–1888						✓	✓
1903–1913		✓		✓		✓	
	1935–1958	✓	✓		✓		✓
2013–2015							✓

Note. The year with every site represents effective starting year of every chronology. BDNP = Bidoup Nui Ba National Park site, the BDNP chronology multiplied by negative one (Buckley *et al.*, 2010); FGY = Fangguangyan site (Guo *et al.*, 2018); GS = Gushan site (Li *et al.*, 2016); MK = sampling site; NML = Niumulin site (Li *et al.*, 2017); RC = regionally composite sites (Duan *et al.*, 2011); XDC04 = a chronology in nearby Zhejiang province (Shi *et al.*, 2015).

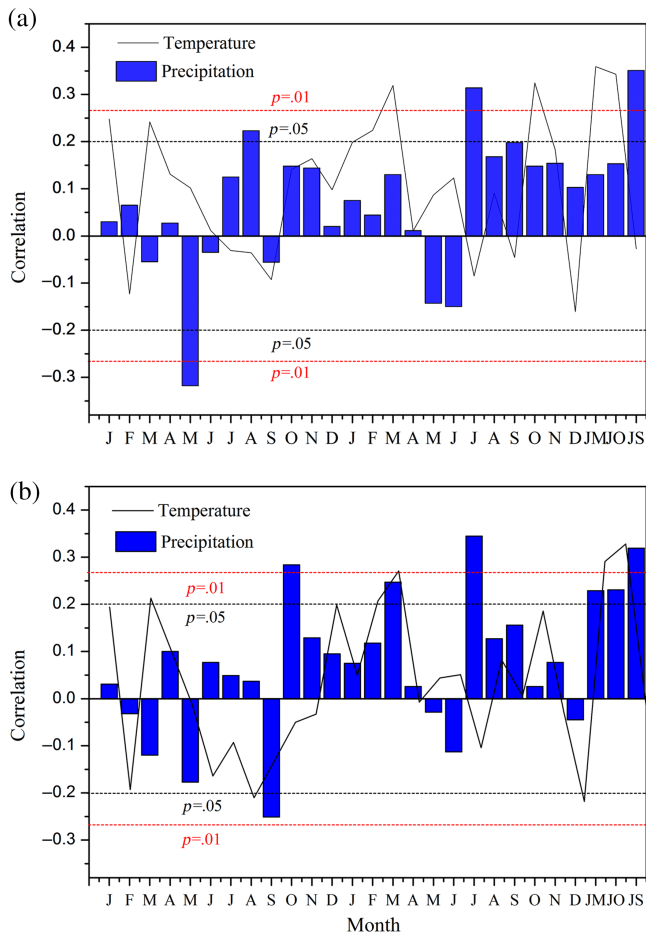


FIGURE 3 Correlations between climate variables and (a) the tree-ring standard chronology, and (b) the first-order differenced tree-ring chronology and the temperature and precipitation from the start of previous growing season (previous February) to the end of current growing season (current December) at Yong'an station for the period of 1954–2015. JM represents the mean from January to March. JO represents the mean from January to October. JS represents the mean from July to September. The black (red) horizontal dashed lines represent the 95% (99%) confidence level [Colour figure can be viewed at wileyonlinelibrary.com]

Apart from significant correlations with SST, positive correlations are seen between our chronology with the GPH at 850 hPa in western Pacific Ocean and negative correlative area centers in the central eastern tropical Pacific Ocean from January to March during 1969–2015 (Figure 5a). This correlation pattern is similar to an El Niño-like pattern, which can result in low (high) GPH in central and eastern (western) tropical Pacific Ocean due to the warm (cold) SST induced upwards (downwards) motion of the air mass (Wang *et al.*, 2013). In the upper-troposphere (at 200 hPa), the tropical trough associated with SST anomalies in the western Pacific expands to the eastern Pacific (Figure 5c). This GPH belt resembles the ENSO circulation model (Yancheva *et al.*, 2007; Fang *et al.*, 2014a; 2014b). The El Niño-like pattern correlation pattern with GPH is more conspicuous for the first-order differenced data (Figure 5b), agreeing with the correlation patterns with SST.

Correlations with oceanic and atmospheric factors suggest that ENSO plays a dominant role on shaping our tree rings. We additionally calculated 21-year window based running correlations with tree-ring chronology to examine their relationships through time. As shown in Figure 6, our tree-ring chronology show high correlations with ENSO indices but the strength of the correlations vary through time. The running correlations with ENSO indices decrease gradually from 1860s to the 1930s, and the correlations increase sharply afterwards reaching a plateau after the 1960s (Figure 6). It is readily understood that the correlations between our tree rings and different ENSO indices are similar as the different ENSO indices are also highly correlated. Moreover, the running correlations with ENSO agree well with the time-varying inter-annual variability as indicated by the changing standard deviations (Figure 6). This indicates that the modulation of ENSO on our tree growth is enhanced in periods with strengthened inter-annual variability.

4 | DISCUSSION

4.1 | Tree growths and local climate conditions

One limiting factor on tree growths at the sampling site is the winter–spring temperature, which has been widely observed in nearby hot and humid regions or remote cold and arid regions in China and surroundings. For example, tree growths are sensitive to winter–spring temperature in Changting (Chen *et al.*, 2012b), in the lower reaches of the Yangtze River (Shi *et al.*, 2010), and in other sites of southeastern and south central China (Duan *et al.*, 2011). This winter–spring temperature limit is also evidenced in cold and humid regions such as *Abies chensiensis* trees in the Jiuzhaigou region of southwest China (Song, 2007), *Pinus koraiensis* trees in Changbai Mountain of northeast China (Zhu *et al.*, 2009) and *Chamaecyparis obtusa* in central Japan (Yonenobu and Eckstein, 2006). In addition, tree growths in cold and arid regions were also found to be limited by temperature in winter–spring, such as *Sabina przewalskii* and *Picea crassifolia* trees on northeast Tibetan Plateau (Liang *et al.*, 2006; Gou *et al.*, 2007; Zhu *et al.*, 2008). These indicate that winter–spring temperature limits growth pattern is a large-scale feature. A cold winter–spring may reduce root and buds activities and even cause damage to them, such as frost desiccation (Pederson *et al.*, 2004; Zhu *et al.*, 2009; Shi *et al.*, 2010). On the other hand, a warm winter–spring can avoid the freezing of leaf tissue ensuring metabolic activity normal (Kimmins, 2005; Chen *et al.*, 2016). Second, a cold winter–spring can delay the beginning of the growing season and thus cause a narrow growth (Shutova *et al.*, 2006; Karlsen *et al.*, 2007).

Although precipitation in the humid study area is generally sufficient for tree growth, it is distributed unevenly and there can be seasonal drought stress for tree growth (Chen

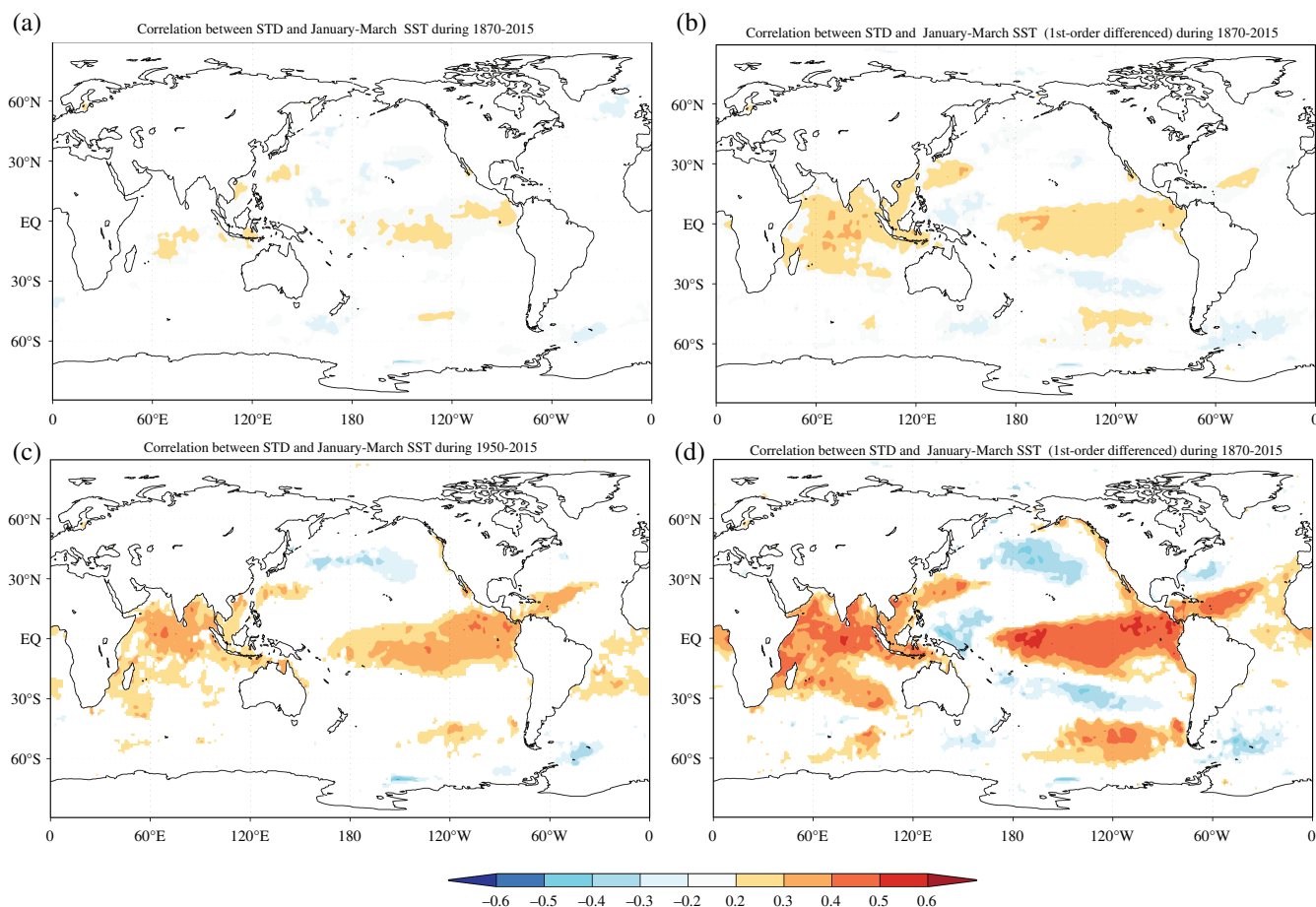


FIGURE 4 Correlations between raw and first-order differenced tree-ring chronologies and sea surface temperatures (SST) from HadISST1 1° reconstruction. (a, b) 1870–2015, (c, d) 1950–2015 [Colour figure can be viewed at wileyonlinelibrary.com]

et al., 2012b). The summer drought limiting growth patterns have been widely observed in nearby sites (Dong *et al.*, 2014; Chen *et al.*, 2016; Li *et al.*, 2016). The precipitation from March to June in the study region accounts for 57.6% of annual precipitation, while precipitation in the hot July and August accounts for only 17% of annual precipitation (Figure S1). Hot and dry summer can intensify soil evaporation and stomatal closure, leading a narrow ring (Wieser and Tausz, 2007; Popa and Kern, 2009; Chen *et al.*, 2012c).

4.2 | Tree growth and ENSO

Similar to the results of many studies in eastern China, the tree-ring is correlated with tropical Pacific sea surface temperature (SST) (Wu *et al.*, 2003; Wang *et al.*, 2000; Zhou and Wu, 2010; Chen *et al.*, 2012b). As an oceanic and atmospheric mode far from the study region, ENSO can only indirectly modulate our tree growth via first causing regional climate anomalies and the regional climate anomalies then leading to growth anomalies. The ENSO causes anomalies of a combination of climate variables and the combination of climate variables happen to be closely related to tree growth. That is, both

ENSO and tree growth are linked to a similar combination of climate variables instead of a single climate variable, such as temperature or precipitation. As revealed above, tree growth is limited by a combination of low winter–spring temperature and dry summer. Indeed, a cold phase of ENSO is often related to a cold winter–spring and a dry summer.

A warm (cold) phase of the ENSO is related to a weak (strong) Walker circulation and thus the retreat of the warm water of the western tropical Pacific Ocean to its eastern part, which is associated with a larger (smaller) warming area of the tropical Pacific Ocean and enhanced (weakened) transport of heat from the tropics to the middle and high latitudes (Fu *et al.*, 2006). Therefore a generally warmer (colder) climate during the warm (cold) phase of the ENSO is expected for the tropical Pacific as whole. This can be particularly the case in winter–spring when the El Niño is in its mature and decay phase. For our study region in southeast China, the winter–spring temperature is strongly modulated by the East Asian winter monsoon. As shown in Figure 5, anomalous high GPH is observed in western Pacific Ocean correspond to an El Niño year. This anticyclone-like pattern

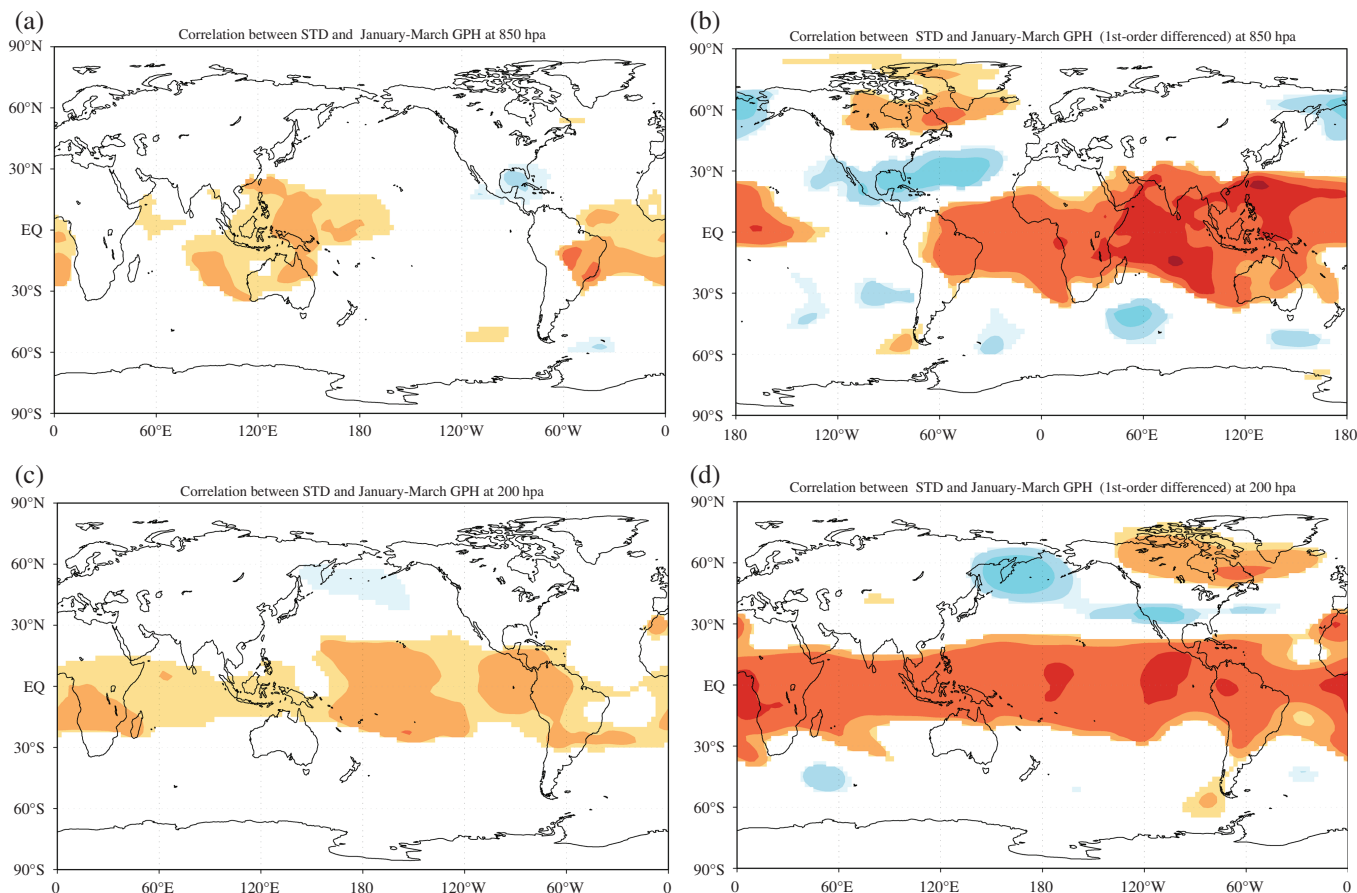


FIGURE 5 Correlations between raw and the first-order differenced chronologies and the geopotential height (GPH) (a, b) at 850 hPa and (c, d) 200 hPa between January and March from the National Centers for Environmental Prediction–National Center for Atmospheric Research (NCEP–NCAR) during 1968–2015 [Colour figure can be viewed at wileyonlinelibrary.com]

in western Pacific Ocean was found to weaken the East Asian winter monsoon (Wang *et al.*, 2000). Both regimes indicate a warm (cold) phase of the ENSO is associated a warm (cold) winter–spring, which can promotes tree growth.

Although ENSO is peak in winter time, its influences on precipitation can be delayed in the coming summer on the East Asian summer monsoon. During the warm phase of the ENSO, high GPH anomalies in western Pacific Ocean are associated with weak upwards motion in the western Pacific Ocean and thus a weak Hadley circulation (Genio, 1997). A weak upwards motion of the western tropical Pacific Ocean can be associated with a weak downwards motion over the western subtropical Pacific Ocean, resulting in a weak western Pacific High. Our sampling site is controlled by the western Pacific High in summer and a weak one can promote precipitation in summer at our study region (Yang and Sun, 2003). In addition, a warm phase of the ENSO is often associated a weak East Asian summer monsoon, which causes a delayed shift of the rain belt from southern to northern China (Huang and Wu, 1989). This can cause a wet southern China, including our study region, and a dry northern China. Tree-ring based study suggested that such a dipole precipitation pattern between southern and northern

China is prominent over the past six centuries, which is mainly regulated by the ENSO (Fang *et al.*, 2014a).

During the mature and decay phase of an El Niño event, a warmer winter–spring (January–March) usually occurs in East Asia (Chen *et al.*, 2012c). Reversely, a cooler winter–

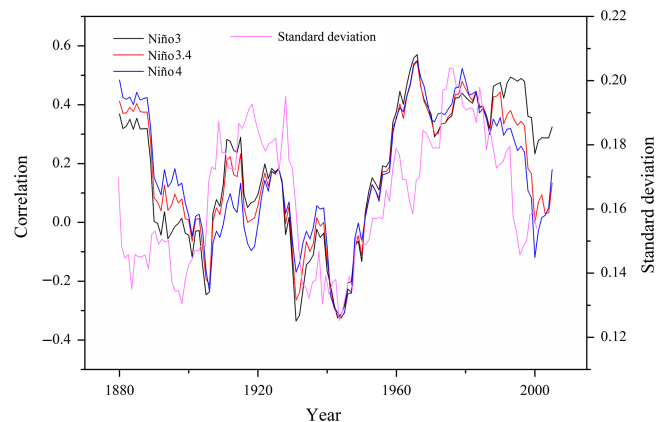


FIGURE 6 Running correlations between the tree-ring chronology and the ENSO indices derived from the Met Office Hadley Centre's sea surface temperature (SST) data set, HadISST1 and the standard deviation of the tree-ring chronology (pink line) based on a 21-year window [Colour figure can be viewed at wileyonlinelibrary.com]

TABLE 3 Comparisons between the El Niño (La Niña) events and winter–spring (January–March) temperatures in Yong’an station since 1954. Temperature anomalies were calculated as the residual of temperatures and naught point 5 SD of the mean (1954–2015) in the study region. El Niño and La Niña events (1954–2015) are based on ENSO monitoring briefing (periods of 18–53) in National Climate Center and some articles (Gergis and Fowler, 2009; Zhang and Zhao, 2012; Zhang *et al.*, 2015)

El Niño year and magnitude classification	Warm winter years	Anomaly (°C)	La Niña years and magnitude classification	Cold winter years	Anomaly (°C)
1965 (strong)	1965	0.73	1955 (strong)	1955	−0.77
1966 (moderate)	1966	1.39	1956 (very strong)	1956	−1.11
1973 (weak)	1973	1.99	1957 (weak)	1957	−1.71
1982 (moderate)	1982	0.73	1962–1963 (weak)	1962–1963	−1.99
1987 (moderate)	1987	2.13	1968 (weak)	1968	−1.61
1991 (moderate)	1978	1.13	1970–1971 (moderate)	1970–1971	−1.19
1997–1998 (very strong)	1997–1998	0.85	1974 (extreme)	1974	−1.57
2002–2003 (weak)	2002–2003	1.61	1984 (moderate)	1984	−1.84
2006–2007 (weak)	2006–2007	1.33	1985–1986 (weak)	1985–1986	−1.39
2009–2010 (strong)	2009–2010	2.06	1995–1996 (moderate)	1995–1996	−0.95
2014–2015 (weak)	2015	1.39			

spring occurs during the mature and decay phase of a La Niña event (Chen, 2002; Kang, 2008; Yuan *et al.*, 2014). We compared years with El Niño (La Niña) events and climate in Yong’an. As shown in Table 3, most of the years with El Niño (La Niña) events correspond to years with warm (cold) winters in the study region. Since 1954, 15 (14) years with El Niño (La Niña) out of 21 (22) years correspond to years with extreme warm (cold) winters with temperature naught point five standard deviation above (below) their mean in the study region (Table 3). The warm winter years (1956, 1966, 1973, 1982, 1987, 1997, 1998 and 2003) were also reported in neighbouring site Changting (Chen *et al.*, 2012b). We share four (1955, 1956, 1957 and 1963) cold winter years out of nine with the reconstruction of Changting since 1954 (Chen *et al.*, 2012b).

Taken together, a warm (cold) phase of the ENSO can cause a warm (cold) winter–spring and a wet (dry) summer in our study region, both of which are favourable climate conditions for tree growth at our site (Kang and Jeong, 1996; Tao and Zhang, 1998). Because the ENSO is most conspicuous on the inter-annual scales, it is expected that its modulation on large-scale climate anomalies is more conspicuous when its inter-annual variability is enhanced. Therefore, the correlations between our tree rings and the ENSO are more conspicuous in recent decades when the ENSO variability is intensified. It is not rare for presence of higher correlations between tree rings and oceanic and atmospheric modes than with single climate variables, which is particularly the case for the hot and humid regions with more than one limiting factor for tree growth. These were termed as “oceanic and atmospheric modes tree-ring chronologies,” such as the chronologies in Himalayan areas (Fang *et al.*, 2017).

To further detect the frequency-dependent relationships between STD and hydroclimate through time in the study area, we calculated the WTC between STD and PDO, AMO. There is common power between STD and PDO on inter-

decadal timescales from 1915 to 1925 (Figure S2a). The WTC plot (Figure S2b) also indicates correlations between STD and AMO from 1854 to 1885 on inter-decadal timescale (Grinsted *et al.*, 2004). However, most periods of the correlation between STD and PDO, AMO appear to be unrelated.

4.3 | Climate change over the past 200 years

Above analyses revealed that the growths of our tree rings are related to winter–spring temperature, summer precipitation and the ENSO. We further study the historical climate signals and its large-scale features, via comparing the extreme years and periods in our tree-ring chronology with nearby tree-ring chronologies in subtropical and tropical parts of the East Asia. We select three chronologies from the same province as our chronology, that is, the closest chronology at Niumulin (NML) site that is sensitive to summer precipitation (Li *et al.*, 2017), two chronologies at Gushan (GS; Li *et al.*, 2016) and Fangguangyan (FGY; Guo *et al.*, 2018) in Fuzhou area that are sensitive to precipitation in summer and autumn precipitation, respectively. We also selected a chronology in nearby Zhejiang province (XDC04) that is controlled by winter–spring precipitation (Shi *et al.*, 2015) and a regionally composite (RC) chronology for nearby Jiangxi and Hunan provinces that is sensitive to winter–spring temperature (Duan *et al.*, 2011). In addition, a well-known chronology from Bidoup Nui Ba National Park (BDNP) in Vietnam that is sensitive to spring (March–May) drought and prior winter (December–February) ENSO is also included for comparisons (Buckley *et al.*, 2010). The BDNP chronology is inversely correlated with prior winter (December–February) ENSO, so the BDNP chronology multiplied by negative one will be used in comparisons (Figure 7). Climate in Vietnam and southeastern China often have reverse responses to ENSO as Vietnam is under the direct control of ENSO, while southeastern China is modulated by ENSO via teleconnections. During the positive

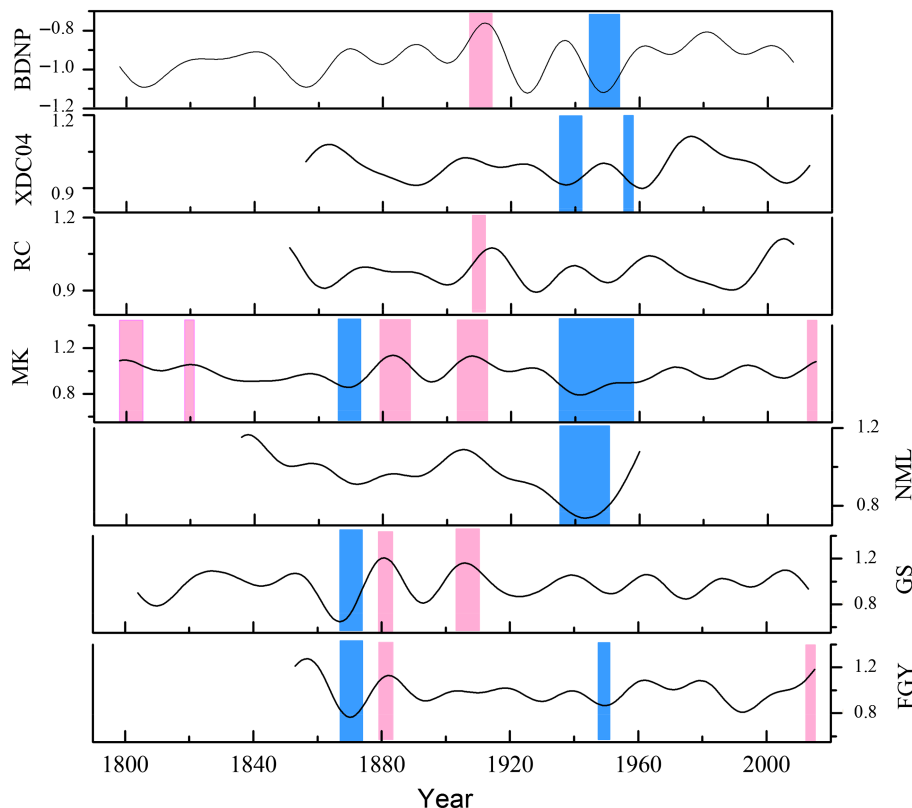


FIGURE 7 Comparison of between the inter-decadal (20 years) variations of our chronology with other chronologies: (a) the Bidoup Nui Ba National Park (BDNP) chronology in the highlands of Vietnam multiplied by negative one (Buckley *et al.*, 2010), (b) the Xiaodai village (XDC04) chronology for the lower reaches of the Yangtze River in southeastern China (Shi *et al.*, 2015), (c) the regionally composite (RC) chronology made from five sampling sites in Jiangxi and Hunan province (Duan *et al.*, 2011), (d) the Makeng (MK) chronology in the study area, (e) the Niumulin (NML) chronology in Quanzhou (Li *et al.*, 2017), (f) the Gushan (GS) chronology near the coastal area of the East China Sea (Li *et al.*, 2016), (g) the Fangguangyan (FGY) chronology in Yongtai, Fujian (Guo *et al.*, 2018). The pink column charts represent consistent positive periods, the blue column charts represent consistent negative periods [Colour figure can be viewed at wileyonlinelibrary.com]

(negative) phase of ENSO, the convective activities in the western Pacific Ocean are suppressed (enhanced), which leads to dry (wet) for regions in its surroundings such as Vietnam (Buckley *et al.*, 2010; Tokinaga *et al.*, 2012). On the other hand, the positive phase (negative) of ENSO is often associated with a southwards (northwards) placement of the western Pacific High, which leads to a delayed (advanced) northwards shift of the rain belt and thus a wet (dry) condition over southeastern China including our study region (Newton *et al.*, 2006; Fang *et al.*, 2014a; Zong, 2017).

The extreme negative growth of our tree rings in year 1870 is found in a nearby tree-ring moisture-sensitive chronology (FGY) in Fuzhou area. It suggests that the extreme low growth at our site may be related to dry conditions (Table 1).

High growth in 1885 appears most widely distributed because it has been revealed in three other tree-ring sites, including tree rings from nearby summer-precipitation-sensitive chronology (FGY) and the moisture-sensitive chronology (XDC04) as well as the composite temperature-sensitive chronology (RC) in southeastern China. Although this chronology mainly reflects temperature, it also has

correlations with precipitation. High growths of our chronology in 1920 and 1987 are only found in moisture-sensitive site (XDC04). These high-growth years correspond to positive anomalies in moisture-sensitive tree rings but match less well with the temperature-sensitive chronology. This suggests that the extremely high growths of our tree rings mainly reflect wet conditions and the wetness in 1885 appear widely spread. It is interesting that our chronology does not share extreme years with the other chronologies (NML and GS chronologies) in Fujian province. It may be because the local-climate signals are different and the disturbance of non-climatic factors while there are mountains and hills in Fujian. Unfortunately, our chronology does not share extreme years with a moisture- and ENSO-sensitive chronology (BDNP) in Vietnam either. This suggests that the years with extreme growths are modulated by climate patterns that have not been extended to southeastern Asia (Table 1).

The extremely low-growth period in our tree rings from 1865–1873 is also found in chronologies from nearby moisture-sensitive sites in Fujian province. The low-growth period in our tree rings from 1935–1958 appears to be more related to large-scale climate anomalies, which have also been found in chronologies of a large area, including nearby

chronologies (NML and FGY) from Fujian province, XDC04 chronology, as well as BDNP chronology (Table 2 and Figure 7). Because both our tree rings and the tree rings from Vietnam are sensitive to the ENSO. This dry epoch may suggest the La Niña-like mode during this period. At the same time, we found the years of 1941–1943 and August 1948 to February 1949 during this epoch are recorded droughty in Zhangping in historical documents (Li, 1995).

Positive growth periods from 1798–1804 and 1819–1821 in our tree rings are not seen in other climate sensitive tree rings because they have not extended back into these periods. The other two high growths periods of 1879–1888 and 2013–2015 are found in nearby moisture-sensitive chronologies (GS and FGY). The high-growth period in our tree rings from 1903 to 1913 has also been found in chronologies of a large area, including nearby GS chronology, a temperature-sensitive chronology (RC) as well as BDNP chronology. Converse to the low-growth period from 1935 to 1958, this wet epoch may suggest the El Niño-like mode during this period. In general, both the low- and high-growth periods corresponding to moisture-sensitive tree rings. Keeping in mind that the extreme years of our tree rings better reflect the moisture changes, we state that the extreme growth years and periods are mainly caused by moisture anomalies. The influence of temperature may cause moderate changes of our tree rings. In addition, it appears that the high-growth periods are less widely distributed than the low-growth periods.

5 | CONCLUSIONS

We developed the first 218-year tree-ring width chronology over the period of 1798–2015 in the Zhangping area in Fujian province, humid subtropical China. The tree growth is positively correlated with winter–spring temperature (January–March) and summer (July–September) precipitation. These climate-growth relationships are widely observed in the southeastern Asia because although the temperature in this subtropical area is high but the cold winter–spring condition can play a limiting role on tree growth. Although it is generally wet in the core area of Asian summer monsoon, the summer precipitation can be low due to the control of the western Pacific High in this time.

Our tree-ring chronology is significantly correlated with ENSO when the ENSO and tree growth are linked to the similar combination of the temperature and precipitation. The linkages between our tree rings and the ENSO are enhanced when the inter-annual variability of the ENSO is increased during the past several decades. As the major regulator of inter-annual climate variability, it is readily understood that its influences can be more conspicuous when its inter-annual variability is enhanced.

The extreme growth years and periods match better with the moisture sensitive chronologies, suggesting that the

precipitation shortages is more likely to cause growth anomalies than temperature. The low-growth period from 1935 to 1958 is the most long-lasting dry period in our chronology, which covers much of the southeastern China. Good matches between our chronology and one ENSO-sensitive chronology in Vietnam suggested the influence of a La Niño-like mode. This dry period in our tree rings corresponds to wet periods in a moisture sensitive chronology in Vietnam, both of which are inversely related to the ENSO.

This study provides one of the longest tree-ring chronologies in southeastern China, one of the core areas of Asian summer monsoon, which can aid in revealing the full picture of dynamics of the Asian summer monsoon.

ACKNOWLEDGEMENTS

We are grateful for the constructive comments from two anonymous reviewers. We thank Prof. Qibing Zhang for sharing the tree-ring data. This research is funded by the National Science Foundation of China (41471172, U1405231 and 91537210), fellowship for the National Youth Talent Support Program of China (Ten Thousand People Plan) and the innovation team project (IRTL1705), the non-profit project of Fujian province (2015R1034-8 and 2015R1034-2). Supports from the Swedish VR, Formas (Future Research Leaders), VINOVA, STINT, BECC, MERGE and SNIC through S-CMIP are also acknowledged.

ORCID

Lei Wang  <https://orcid.org/0000-0003-2156-3657>

REFERENCES

- Allan, R., Lindesay, J., & Parker, D. (1996). *El Niño: Southern Oscillation and Climatic Variability*. Collingwood, Vic.: CSIRO Publishing.
- Buckley, B.M., Anchukaitis, K.J., Penny, D., Fletcher, R., Cook, E.R. and Sano, M. (2010) Climate as a contributing factor in the demise of Angkor, Cambodia. *Proceedings of the National Academy of Sciences of the United States of America*, 107(15), 6748–6752. <https://doi.org/10.1073/pnas.0910827107>.
- Chen, W. (2002) Impacts of El Niño and La Niña on the cycle of the East Asian winter and summer monsoon. *Chinese Journal of Atmospheric Sciences*, 26(5), 595–610.
- Chen, F., Yuan, Y.J., Wei, W.S., Yu, S.L. and Zhang, T.W. (2012a) Reconstructed temperature for Yong'an, Fujian, southeast China: linkages to the Pacific Ocean climate variability. *Global and Planetary Changes*, 86–87, 11–19. <https://doi.org/10.1016/j.gloplacha.2012.01.005>.
- Chen, F., Yuan, Y.J., Wei, W.S., Yu, S.L. and Zhang, T.W. (2012b) Tree ring-based winter temperature reconstruction for Changting, Fujian, subtropical region of southeast China, since 1850: linkages to the Pacific Ocean. *Theoretical and Applied Climatology*, 109(1–2), 141–151. <https://doi.org/10.1007/s00704-011-0563-0>.
- Chen, F., Yuan, Y., Wen, W., Yu, S., Fan, Z. and Zhang, R. (2012c) Tree-ring-based reconstruction of precipitation in the Changling Mountains, China, since A.D.1691. *International Journal of Biometeorology*, 56(4), 765–774. <https://doi.org/10.1007/s00484-011-0431-8>.
- Chen, F., Yuan, Y., Wei, W., Yu, S. and Wang, H. (2015) Tree-ring response of subtropical tree species in southeast China on regional climate and sea-surface temperature variations. *Trees*, 29(1), 17–24. <https://doi.org/10.3969/j.issn.1001-7410.2011.01.13>.

- Chen, D., Fang, K.Y., Li, Y.J., Dong, Z.P., Zhang, Y. and Zhou, F.F. (2016) Response of *Pinus taiwanensis* growth to climate changes at its southern limit of Daiyun Mountain, mainland China Fujian province. *Science China Earth Sciences*, 59(2), 328–336. <https://doi.org/10.1007/s11430-015-5188-1>.
- Cook, E. (1985) *A time series analysis approach to tree ring standardization*. PhD Thesis, University of Arizona, Tucson.
- Cook, E.R., Krusic, P.J. and Jones, P.D. (2003) Dendroclimatic signals in long tree-ring chronologies from the Himalayas of Nepal. *International Journal of Climatology*, 23(7), 707–732. <https://doi.org/10.1002/joc.911>.
- Dong, Z.P., Zheng, H.Z., Fang, K.Y., Yan, R., Zheng, L.W. and Yang, Y.S. (2014) Responses of tree-ring width of *Pinus massiniana* to climate change in Sanming, Fujian province. *Journal of Subtropical Resources and Environment*, 9(1), 1–7.
- Du, Y. and Xie, S.P. (2008) Role of atmospheric adjustments in the tropical Indian Ocean warming during the 20th century in climate models. *Geophysical Research Letters*, 35(8), 193–202. <https://doi.org/10.1029/2008GL033631>.
- Duan, J., Zhang, Q.B., Lv, L. and Zhang, C. (2011) Regional-scale winter-spring temperature variability and chilling damage dynamics over the past two centuries in southeastern China. *Climate Dynamics*, 39(3–4), 919–928. <https://doi.org/10.1007/s00382-011-1232-9>.
- Fang, K., Chen, D., Li, J. and Seppä, H. (2014a) Covarying hydroclimate patterns between monsoonal Asia and North America over the past 600 years. *Journal of Climate*, 27(21), 8017–8033. <https://doi.org/10.1175/JCLI-D-13-00364.1>.
- Fang, K., Wilkening, M., Davi, N., Zhou, F. and Liu, C. (2014b) An ensemble weighting approach for dendroclimatology: drought reconstructions for the northeastern Tibetan Plateau. *Plos One*, 9(1), e86689. <https://doi.org/10.1371/journal.pone.0086689>.
- Fang, K., Seppä, H. and Chen, D. (2015) Interdecadal hydroclimate teleconnections between Asia and North America over the past 600 years. *Climate Dynamics*, 44(7–8), 1777–1787. <https://doi.org/10.1007/s00382-014-2266-6>.
- Fang, K., Guo, Z., Chen, D., Linderholm, H.W., Li, J., Zhou, F., Guo, G., Dong, Z. and Li, Y.J. (2017) Drought variation of western Chinese Loess Plateau since 1568 and its linkages with droughts in western North America. *Climate Dynamics*, 49, 1–12. <https://doi.org/10.1007/s00382-017-3545-9>.
- Fu, Q., Johanson, C.M., Wallace, J.M. and Reichler, T. (2006) Enhanced mid-latitude tropospheric warming in satellite measurements. *Science*, 312(5777), 1179. <https://doi.org/10.1126/science.1125566>.
- Genio, A.D.D. (1997) *Hadley Circulation*. Encyclopedia of Earth Science. https://doi.org/10.1007/1-4020-4520-4_164.
- Gergis, J.L. and Fowler, A.M. (2009) A history of ENSO events since A.D. 1525: implications for future climate change. *Climatic Change*, 92(3–4), 343–387. <https://doi.org/10.1007/s10584-008-9476-z>.
- Gou, XH, Chen, FH., Jacoby, G., Cook, ER., Yang, MX. Peng, JF. and Zhang Y. (2007) Rapid tree growth with 500 respect to the last 400 years in response to climate warming, northeastern Tibetan plateau. *International Journal of Climatology*, 27(11), 1497–1503. <https://doi.org/10.1002/joc.1480>.
- Gou, X., Deng, Y., Gao, L., Chen, F., Cook, E., Yang, M.X. and Zhang, F. (2015) Millennium tree-ring reconstruction of drought variability in the eastern Qilian Mountains, northwest China. *Climate Dynamics*, 45(7–8), 1761–1770. <https://doi.org/10.1007/s00382-014-2431-y>.
- Grinsted, A., Moore, J.C. and Jevrejeva, S. (2004) Application of the cross wavelet transform and wavelet coherence to geophysical time series. *Nonlinear Processes in Geophysics*, 11(5/6), 561–566. <https://doi.org/10.5194/npg-11-561-2004>.
- Guo, G.Y., Fang, K.Y., Li, J.B., Linderholm, H.W., Li, D.W., Zhou, F.F., Dong, Z.P., Li, Y.G. and Wang L. (2018) Increasing intrinsic water-use efficiency over the past 160 years does not stimulate tree growth for a drought stressed site in the western bank of Taiwan Strait. *Climate Research*. <https://doi.org/10.3354/cr01526>.
- Hartmann, D.L., Tank, A.M. and Rusticucci, M. (2013) *IPCC Fifth Assessment Report, Climate Change: The Physical Science Basis*. Cambridge and New York: Cambridge University Press.
- Holmes, R.L. (1983) Computer-assisted quality control in tree-ring dating and measurement. *Tree-Ring Bulletin*, 44(3), 69–75. <https://doi.org/10.1007/BF02656915>.
- Huang, R. and Wu, Y. (1989) The influence of ENSO on the summer climate change in China and its mechanism. *Advances in Atmospheric Sciences*, 6(1), 21–32.
- Kalnay, E., Kanamitsu, M., Kistler, R., Collins, W., Deaven, D., Gandin, L., Iredell, M., Saha, S., White, G., Woollen, J., Zhu, Y., Leetmaa, A., Reynolds, R., Chelliah, M., Ebisuzaki, W., Higgins, W., Janowiak, J., Mo, K.C., Ropelewski, C., Wang, J., Roy Jenne, Dennis Joseph. (1996) The NCEP/NCAR 40-year reanalysis project. *Bulletin of the American Meteorological Society*, 77(3), 437–472. [https://doi.org/10.1175/1520-0477\(1996\)077<0437: TNYRP>2.0.CO;2](https://doi.org/10.1175/1520-0477(1996)077<0437: TNYRP>2.0.CO;2).
- Kang, S.G. (2008) Impacts of a La Niña on the climate in China. *The Central Plains Culture Research*, 16(3), 242–242.
- Kang, I.S. and Jeong, Y.K. (1996) Association of interannual variations of temperature and precipitation in Seoul with principal modes of Pacific SST. *Asia-Pacific Journal of Atmospheric Sciences*, 32(4), 1–17.
- Karlsen, S.R., Solheim, I., Beck, P.S., Høgda, K.A., Wielgolaski, F.E. and Tømmervik, H. (2007) Variability of the start of the growing season in Fennoscandia, 1982–2002. *International Journal of Biometeorology*, 51(6), 513–524. <https://doi.org/10.1007/s00484-007-0091-x>.
- Kennedy, J.J., Rayner, N.A., Smith, R.O., Parker, D.E. and Saunby, M. (2011) Reassessing biases and other uncertainties in sea-surface temperature observations since 1850: 2: biases and homogenization. *Journal of Geophysical Research: Atmospheres*, 116(D14), D14104. <https://doi.org/10.1029/2010JD015220>.
- Kimmins, J.P. (2005) *Forest Ecology*, Vol. 258. Beijing: China Forestry Publishing House, pp. 17–43. <https://doi.org/10.1002/9780470995242.ch2>.
- Li, Z.F. (1995) *Zhangping County Annals*. Shanghai: Sanlian Store.
- Li, Y., Fang, K., Cao, C., Li, D., Zhou, F., Dong, Z., Zhang, Y. and Gan, Zh. (2016) A tree-ring chronology spanning the past 210 years in the coastal area of Southeast China and its relationship with climate change. *Climate Research*, 67(3), 209–220. <https://doi.org/10.3354/cr01376>.
- Li, D., Fang, K., Li, Y., Chen, D., Liu, X., Dong, Z., Zhou, F., Guo, G., Shi, F., Xu, C. and Li, Y. (2017) Climate, intrinsic water-use efficiency and tree growth over the past 150 years in humid subtropical China. *Plos One*, 12(2), e0172045. <https://doi.org/10.1371/journal.pone.0172045>.
- Liang, E., Shao, X., Eckstein, D., Lei, H. and Liu, X. (2006) Topography- and species-dependent growth responses of *Sabina przewalskii* and *Picea crassifolia* to climate on the northeast Tibetan Plateau. *Forest Ecology and Management*, 236(2), 268–277. <https://doi.org/10.1016/j.foreco.2006.09.016>.
- Liu, Y., Wang, Y., Li, Q., Song, H., Linderholm, H.W., Leavitt, S.W., Leavitt, S.W., Wang, R. and An, Z. (2015) Tree-ring stable carbon isotope-based May–July temperature reconstruction over Nanwutai, China, for the past century and its record of 20th century warming. *Quaternary Science Reviews*, 93, 67–76. <https://doi.org/10.1016/j.quascirev.2014.03.023>.
- Newton, A., Thunell, R. and Stott, L. (2006) Climate and hydrographic variability in the Indo-Pacific warm pool during the last millennium. *Geophysical Research Letters*, 33(19), L19710. <https://doi.org/10.1029/2006GL027234>.
- Pederson, N., Cook, E.R., Jacoby, G.C., Peteet, D.M. and Griffin, K.L. (2004) The influence of winter temperatures on the annual radial growth of six northern range margin tree species. *Dendrochronologia*, 22(1), 7–29. <https://doi.org/10.1016/j.dendro.2004.09.005>.
- Popa, I. and Kern, Z. (2009) Long-term summer temperature reconstruction inferred from tree-ring records from the eastern Carpathians. *Climate Dynamics*, 32(7–8), 1107–1117. <https://doi.org/10.1007/s00382-008-0439-x>.
- Rayner, N.A., Parker, D.E., Horton, E.B., Folland, C.K., Alexander, L.V., Rowell, D.P., Kent, E.C., Kaplan, A. (2003) Global analyses of sea surface temperature, sea ice, and night marine air temperature since the late nineteenth century. *Journal of Geophysical Research: Atmospheres*, 108(D14), 1063–1082. <https://doi.org/10.1029/2002JD00267>.
- Shao, X., Xu, Y., Yin, Z.Y., Liang, E., Zhu, H. and Wang, S. (2010) Climatic implications of a 3585-year tree-ring width chronology from the northeastern Qinghai–Tibetan Plateau. *Quaternary Science Reviews*, 29(17–18), 2111–2122. <https://doi.org/10.1016/j.quascirev.2010.05.005>.
- Shi, J.F., Cook, E.R., Lu, H.Y., Li, J.B., Wright, W.E. and Li, S.F. (2010) Tree-ring based winter temperature reconstruction for the lower reaches of the Yangtze River in southeast China. *Climate Research*, 41(2), 169–176. <https://doi.org/10.3354/cr00851>.
- Shi, J.F., Lu, H.Y., Li, J.B., Shi, S.Y., Wu, S., Hou, X. and Li, L.L. (2015) Tree-ring based February–April precipitation reconstruction for the lower reaches of the Yangtze River, southeastern China. *Global and Planetary Change*, 131, 82–88. <https://doi.org/10.1016/j.gloplacha.2015.05.006>.
- Shutova, E., Wielgolaski, F.E., Karlsen, S.R., Makarova, O., Berlina, N., Filimonova, T., Haraldsson, E., Aspholm, P.E., Flø, L. and Høgda, K.A. (2006) Growing seasons of Nordic mountain birch in northernmost Europe

- as indicated by long-term field studies and analyses of satellite images. *International Journal of Biometeorology*, 51(2), 155–166. <https://doi.org/10.1007/s00484-006-0042-y>.
- Song, H. (2007) Winter mean lowest temperature derived from tree-ring width in Jiuzhaigou region, China since 1750A.D. *Quaternary Sciences*, 27(4), 486–491.
- Stokes, M.A. and Smiley, T.L. (1968) *An Introduction to Tree-Ring Dating*. Tucson: University of Arizona Press.
- Sturman, A. (2010) El Niño–Southern Oscillation and climatic variability. *New Zealand Geographer*, 54(1), 64–65. <https://doi.org/10.1111/j.1745-7939.1998.tb00534.x>.
- Tao, S.Y. and Zhang, Q.Y. (1998) Response of the East Asian summer monsoon to ENSO events. *Scientia Atmospherica Sinica*, 22, 399–407 (in Chinese). <https://doi.org/10.3878/j.issn.1006-9895.1998.04.02>.
- Tokenaga, H., Xie, S.P., Deser, C., Yu, K. and Okumura, Y.M. (2012) Slowdown of the Walker circulation driven by tropical Indo-Pacific warming. *Nature*, 491(7424), 439–443. <https://doi.org/10.1038/nature11576>.
- Wang, B., Wu, R. and Fu, X. (2000) Pacific–East Asian teleconnection: how does ENSO affect East Asian climate? *Journal of Climate*, 13(9), 1517–1536. [https://doi.org/10.1175/1520-0442\(2000\)013<1517:PEATHD2.0.CO;2](https://doi.org/10.1175/1520-0442(2000)013<1517:PEATHD2.0.CO;2).
- Wang, X., Brown, P.M., Zhang, Y. and Song, L. (2011) Imprint of the Atlantic Multidecadal Oscillation on tree-ring widths in northeastern Asia since 1568. *Plos One*, 6(7), e22740. <https://doi.org/10.1371/journal.pone.0022740>.
- Wang, C., Xie, S.P. and Carton, J.A. (2013) Westerly wind events in the tropical Pacific and their influence on the coupled ocean–atmosphere system: a review. *Earth's Climate*, 147, 49–69. <https://doi.org/10.1029/147GM03>.
- Wieser, G. and Tausz, M. (2007) *Trees at Their Upper Limit: Treelife Limitation at the Alpine Timberline*, Vol. 5. Dordrecht, The Netherlands: Springer Science & Business Media, p. 232. https://doi.org/10.1007/1-4020-5074-7_1.
- Wigley, T.M.L., Briffa, K.R. and Jones, P.D. (1984) On the average value of correlated time series, with applications in dendroclimatology and hydrometeorology. *Journal of Climatology & Applied Meteorology*, 23(2), 201–213. [https://doi.org/10.1175/1520-0450\(1984\)023<0201:OTAVOC>2.0.CO;2](https://doi.org/10.1175/1520-0450(1984)023<0201:OTAVOC>2.0.CO;2).
- Wu, R., Hu ZZ, Kirtman BP. (2003) Evolution of ENSO-related rainfall anomalies in east Asia. *Journal of Climate*, 16(22), 3742–3758. <https://doi.org/10.1175/1520-0442>.
- Xie, S.P., Xie, Q., Wang, D. and Liu, W.T. (2003) Summer upwelling in the South China Sea and its role in regional climate variations. *Journal of Geophysical Research: Oceans*, 108(C8), 3261. <https://doi.org/10.1029/2003JC001867>.
- Xie, S.P., Yan, D., Gang, H., Zheng, X.T., Tokenaga, H., Hu, K.M. and Liu, Q. Y. (2010) Decadal shift in El Niño influences on Indo-Western Pacific and East Asian climate in the 1970s. *Journal of Climate*, 23(12), 3352–3368. <https://doi.org/10.1175/2010JCLI3429.1>.
- Yancheva, G., Nowaczyk, N.R., Mingram, J., Dulski, P., Schettler, G., Negendank, J.F., Liu, J.Q., Sigman, D.M., Peterson, L.C. and Haug, G.H. (2007) Influence of the Intertropical Convergence Zone on the East Asian monsoon. *Nature*, 445(7123), 74–77. <https://doi.org/10.1038/nature05431>.
- Yang, H. and Sun, S.Q. (2003) Longitudinal displacement of the subtropical high in the western Pacific in summer and its influence. *Advances in Atmospheric Sciences*, 20(6), 921–933. <https://doi.org/10.1007/BF02915515>.
- Yang, S., Lau, K.M. and Kim, K.M. (2002) Variations of the East Asian jet stream and Asian–Pacific–American winter climate anomalies. *Journal of Climate*, 15(15), 306–325. [https://doi.org/10.1175/1520-0442\(2002\)015<0306:VOTEAJ>2.0.CO;2](https://doi.org/10.1175/1520-0442(2002)015<0306:VOTEAJ>2.0.CO;2).
- Yang, B., Qin, C., Wang, J., He, M., Melvin, T.M. and Osborn, T.J. (2014) A 3,500-year tree-ring record of annual precipitation on the northeastern Tibetan Plateau. *Proceedings of the National Academy of Sciences of the United States of America*, 111, 2903–2908, 2908. <https://doi.org/10.1073/pnas.1319238111>.
- Yonenobu, H. and Eckstein, D. (2006) Reconstruction of early spring temperature for central Japan from the tree-ring widths of Hinoki cypress and its verification by other proxy records. *Geophysical Research Letters*, 33(10), 328–340. <https://doi.org/10.1029/2006GL026170>.
- Yuan, Y., Li, C.Y. and Yang, S. (2014) Decadal anomalies of winter precipitation over southern China in association with El Niño and La Niña. *Journal of Meteorological Research*, 28(1), 91–110. <https://doi.org/10.1007/s13351-014-0106-6>.
- Zhang, P. and Zhao, J. (2012) The influence of El Niño/La Niña events on climate of Shanxi Province. *Journal of Arid Land Resources and Environment*, 26(2), 74–78.
- Zhang, Q.B., Evans, M.N. and Lyu, L. (2015) Moisture dipole over the Tibetan Plateau during the past five and a half centuries. *Nature Communications*, 6, 8062. <https://doi.org/10.1038/ncomms9062>.
- Zhou, L.T. and Wu, R. (2010) Respective impacts of the East Asian winter monsoon and ENSO on winter rainfall in China. *Journal of Geophysical Research: Atmospheres*, 115(D2), D02107. <https://doi.org/10.1029/2009JD012502>.
- Zhu, H.F., Zheng, Y.H., Shao, X.M., Liu, X.H., Yan, X. and Liang, E.Y. (2008) Millennial temperature reconstruction based on tree-ring widths of Qilian juniper from Wulan, Qinghai province, China. *Chinese Science Bulletin*, 53(24), 3914–3920. <https://doi.org/10.1007/s11434-008-0400-8>.
- Zhu, H.F., Fang, X.Q., Shao, X.M. and Yin, Z.Y. (2009) Tree ring-based February–April temperature reconstruction for Changbai mountain in northeast China and its implication for East Asian winter monsoon. *Climate of the Past Discussions*, 5(2), 661–666. <https://doi.org/10.5194/cp-5-661-2009>.
- Zong, H.F. (2017) Seasonal evolutions of two typical seasons and its relationship with precipitation in eastern China. *Chinese Journal of Atmospheric Sciences*, 6(6), 1264–1283 (in Chinese).

SUPPORTING INFORMATION

Additional supporting information may be found online in the Supporting Information section at the end of the article.

How to cite this article: Wang L, Fang K, Chen D, et al. Intensified variability of the El Niño–Southern Oscillation enhances its modulations on tree growths in southeastern China over the past 218 years. *Int J Climatol*. 2018;38:5293–5304. <https://doi.org/10.1002/joc.5730>